Motion control of urea powered biocompatible hollow microcapsules

Xing Ma[‡], *Xu Wang*[‡], *Kersten Hahn*[†] *and Samuel Sanchez*[*,‡,§,‖]

[‡] Max Planck Institute for Intelligent Systems Institution, Heisenbergstraße 3, 70569 Stuttgart, Germany.

[†] Stuttgart Center for Electron Microscopy, Max Planck Institute for Solid State Research, Heisenbergstraße 1, 70569 Stuttgart, Germany.

[§] Institució Catalana de Recerca i EstudisAvancats (ICREA), Pg. Lluís Companys 23, 08010, Barcelona, Spain

[‖] Institut de Bioenginyeria de Catalunya (IBEC), Baldiri I Reixac 10-12, 08028 Barcelona, Spain

KEYWORDS: Microcapsule motor, directional self-propulsion, motion control, enzymatic motor, mesoporous silica

ABSTRACT: The quest for fully biocompatible micro-swimmers with capability of long-range directional self-propulsion and controllable motion is a long-standing challenge in the field of active matter, but of great significance in biomedical applications. Here, we present an active hybrid microcapsule motor based on Janus hollow mesoporous silica micro particles (JHP) powered by the bio-catalytic decomposition of urea at physiological concentrations. The

directional self-propelled motion lasts longer than 10 minutes with an average velocity of up to 6 body lengths per second. Additionally, we control the velocity of the micro-motor by chemically inhibiting and reactivating the enzymatic activity of urease. The incorporation of magnetic material within the Janus structure provides remote magnetic control on the movement direction. Furthermore, the mesoporous/hollow structure can load both small molecules and larger particles up to hundreds of nano-meters, making the hybrid micro-motor as an active and controllable drug delivery micro-system.

Current tools of nanotechnology allow for the engineering of matter at the micro and nano scales with a high degree of structural and morphological control. Recently, researchers have investigated possible strategies to provide these structures with "life" in the form of self-propulsion, aiming at "micro/nano-machines" that can convert chemical energy into kinetic energy providing self-propelled motion.[1] Biomedical applications of micro/nano-machines, such as targeted drug delivery, have been dreamed by the community for long.[2] However, the entire efforts of miniaturizing machines becomes futile if non-biocompatible fuels are used to power these artificial micro/nano-machines, e.g. Pt/H_2O_2, the most widely used agent to induce self-propulsion.[3] While alternatives to Pt/H_2O_2 have been suggested in the literature,[4] they all suffer from different drawbacks such as toxic reaction reagents,[4a, 4c, 4f, 4g] a short life-time,[4d, 4e] or requiring extreme reaction conditions.[4b] The major remaining challenge is thus to find biocompatible micro/nano-machines that are capable of autonomous motion. As a first step to overcome this challenge, the micro/nano-machines must be composed of biocompatible and -degradable materials and should "consume" non-toxic fuels - ideally available as biological fluids - to facilitate sustained self-propulsion.

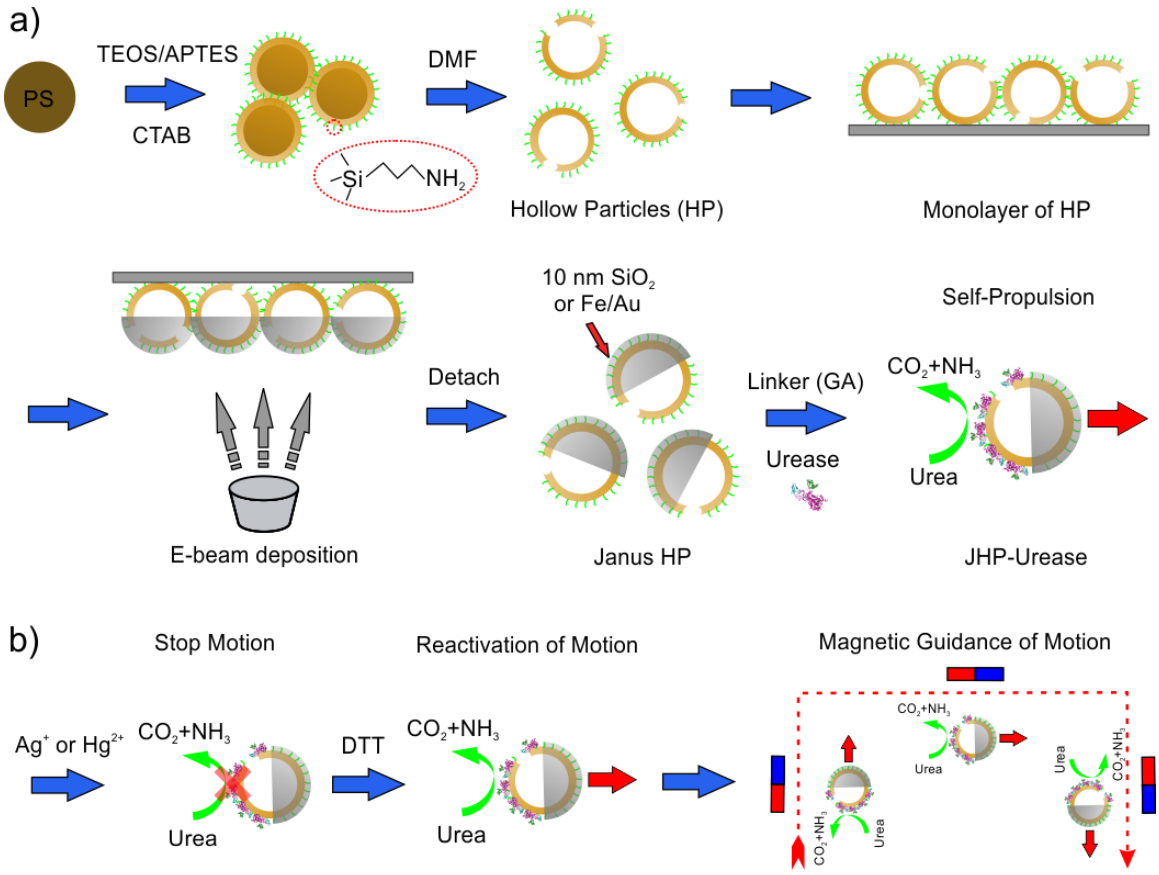

Figure 1. Schematic illustrating a) the fabrication of a urea driven active hybrid microcapsule motor; b) motion control on the microcapsule by chemically inhibiting/reactivating the enzymatic activity of urease, and remote magnetic guidance on the movement direction of the micro-motor. (TEOS: tetraethylorthosilicate; APTES: 3-aminopropyltriethoxysilane; CTAB: cetyltrimethylammonoium bromide; DMF: dimethylformamide; DTT: dithiothreitol.)

In virtue of versatile enzyme/fuel choices, enzymes triggered bio-catalytic reactions have been regarded as promising alternatives to address the biocompatibility issue of these micro/nano-motors. In previous reports, researchers used catalase to replace Pt and pushed the micro-tubes[5] or particles[6] by bubble propulsion, but the systems were still fueled by toxic and strongly oxidative H_2O_2. There were reports of other enzymes being capable to act as active nano-

motors,[7] or of enzymes having been immobilized onto micro/nano objects for mechanical pumping[8] or active motion,[9] Very recently, researchers proved the possibility of using enzymes and biocompatible fuels to power self-propelled micro/nano-motors, demonstrated as enhanced diffusion or accelerated random walk of those enzyme conjugated micro/nano particles.[10] However, long-range directional self-propulsion of enzyme powered micro/nano-motors consuming biocompatible fuel has not been achieved by current systems yet. Furthermore, once these active motors are strong enough to overcome Brownian diffusion, they should allow for motion control including velocity variation and directional guidance, enabling them to move towards particular target locations on demand.

Here, we accomplish such a target and present the design and fabrication of biocompatible micro-capsule motors based on Janus hollow mesoporous silica micro-particle (JHP) (**Figure 1**). Mesoporous silica was reported to be biocompatible and has been widely investigated as a theranostic platform in the nano/micro size range.[11] A micro-motor made of mesoporous silica is therefore expected to be biocompatible in a physiological environment. Given the fact that the surface chemistry of silica is well understood,[12] we could bind the enzyme urease to trigger the bio-catalytic reaction of decomposition of urea into CO_2 and NH_3 (Figure 1a), and provided the mechanical driving force to the hybrid microcapsule through a chemo-phoretic mechanism. By chemically manipulating the enzymatic activity of urease with the inhibitors, e.g. Ag^+ or Hg^{2+}, and the thiol protection reagent dithiothreitol (DTT),[13] we achieved control over the velocity of the microcapsule (Figure 1b). We could also implement an instant "on/off" switch on the motion of the microcapsule through the rapid and sequential addition of inhibitors ("off") or DTT ("on"). In addition to velocity control by altering the power output of the enzymatic "engine", the deposition of a magnetic element (Fe) onto the Janus particle allowed us to achieve directional guidance on

the micro-motor. To the best of our knowledge, this is the first successful demonstration of using a single enzyme with biological fuel in combination with chemical methods and remote magnetic fields to achieve fully controlled long-range directional motion of a biocompatible Janus micro-motor. Given the biocompatible nature, the complete motion control, and the ability to add multiple cargo loads, we expect the active microcapsule to be able to fulfill cargo delivery tasks on-demand, providing new solutions for targeted drug delivery in biomedical research and applications.

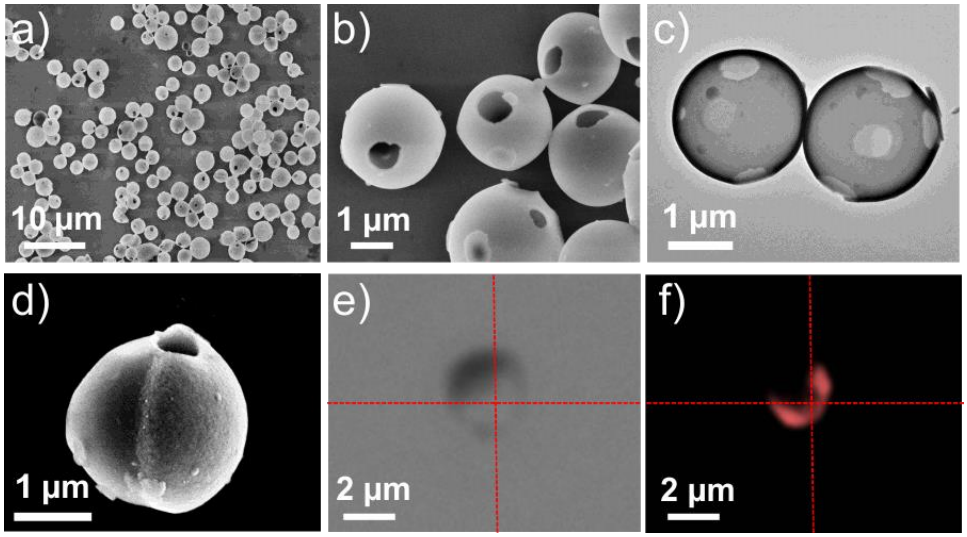

Figure 2. Characterization of the mesoporous silica micro HP, JHP and JHP-Urease. SEM images of the HP at a) low and b) high magnification; c) TEM image of the HP; d) SEM image of the JHP half coated with Fe(10nm)/Au(3nm); e) bright field and f) fluorescence (E_x/E_m=520/580 nm) images of JHP-Urease micro-capsule stained by Krypton protein staining dye. The dark part in (e) indicates the metallic coating side of the JHP-Urease. The red color in (f) indicates the position of the stained enzyme urease. The dotted red lines in (e) and (f) indicate the position of the Janus particle.

Polystyrene (PS) micro-particles (about 2.3 μm in diameter) were used as templates for the fabrication of the HP following a previously reported method[14] which was slightly modified by pre-functionalizing the HP with amine groups (-NH_2) using the co-condensation method (Figure 1a) (see Experimental Section in the Supporting Information(SI)). We characterized the HP by scanning electron microscopy (SEM) (Figure 2a and b). The diameters of the particles were found to be 2.32±0.03 μm (average ± standard error of mean, N=30). Transmission electron microscopy (TEM) revealed the hollow structure of the micro-particles, evidenced by the bright contrast of the hollow cavity containing black circular rings (Figure 2c). The presence of mesopores in the shell of the HP was observed by TEM (Figure S1 in the SI). The specific surface area of the mesoporous HP was found to be 1.284×10^3 m^2 g^{-1} by N_2 adsorption/desorption measurement with typical type IV isotherm curves (Figure S2a in the SI). The internal diameter of the mesopores was about 2.17 nm as indicated by the Barrett-Joyner-Halenda (BJH) desorption pore size distribution curve (Figure S2b in the SI). We sometimes observed large holes with average diameters of 0.540±0.03 μm (average±standard error of mean, N=10) on the particle surface (Figure 2a, b and c). From the orifices of the pores, the average shell thickness of the HP was measured to be 77±4 nm (average±standard error of mean, N=10). The formation of these large holes can be attributed to the attachment between particles during the "sol-gel" growth of the shell of mesoporous silica. The circular shell area that was in contact with other particles was further pulled off by mechanical force due to strong vortex treatment during the washing process. The "pore opening" on the mesoporous silica shell also facilitated the dissolution and removal of the PS template by DMF.

The Janus architecture was achieved by e-beam deposition of SiO_2 (10nm) or Fe(10nm)/Au(3nm) (for remote magnetic control). For an improved visualization of the Janus

structure, the Janus microcapsule half-coated with the metallic elements (Fe/Au) were observed under SEM (Figure 2d), which clearly showed the asymmetric coating with Fe/Au present on the right hemisphere only. Enzyme urease was immobilized onto the non-coated side of the JHP by using glutaraldehyde (GA) as a linker molecule.[15] The urease conjugated Janus hollow particle, denoted as JHP-Urease, was qualitatively characterized by UV-vis adsorption (Figure S3 in the SI) and circular dichroism (CD) spectra (Figure S4 in the SI). Compared to free urease which has an adsorption peak at 280 nm, the JHP-Urease shows its adsorption peak at 268 nm. The associated blue-shift of 12 nm can be explained by the configurational change of the urease after immobilization,[16] which was further confirmed by the signal loss at 222 nm in the CD spectra suggesting a decrease of α–helical content due to the partial unfolding of urease during chemical conjugation.[17] Quantitatively, the amount of urease conjugated to the JHP was calculated as 14.95±1.10 μg per mg hollow particles (average ± standard error of mean, N=4) by using the Coomassie Brilliant Blue (CBB) based protein quantification kit (Figure S5 and Table S1 in the SI). In order to directly visualize the asymmetric presence of urease, we used a commercial protein staining dye (Krypton™ Protein Stain) to stain the JHP-Urease before examining the sample under florescence microscopy. Under bright field illumination, the Janus structure is revealed by the difference in contrast between the metallic coating layer (dark) and the mesoporous silica shell (bright) (Figure 2e). After switching to the fluorescence channel, we observed the red fluorescence emission due to the binding of the dye to the protein urease, indicating the Janus distribution of urease on the non-coated hemisphere (Figure 2f). The fabrication and functionalization of the JHP-Urease was followed by a zeta-potential measurement (Figure S6 in the SI). Prior to e-beam deposition, the HP presented a high positive surface charge of 57.6±7.0 mV (average ± standard deviation, N=10) due to the positive charge

of protonated amine groups present on the particle surface. This value decreased to 27.6±5.7 mV (average ± standard deviation, N=10) after e-beam deposition of SiO_2, which is close to the theoretical ideal of half the amine groups being covered by non-functionalized amorphous silica. The zeta-potential of JHP-Urease shifted to negative values of -24.3±4.3 mV (average ± standard deviation, N=10) after functionalizing with urease, confirming the partial coverage of the particle's surface with enzymes.

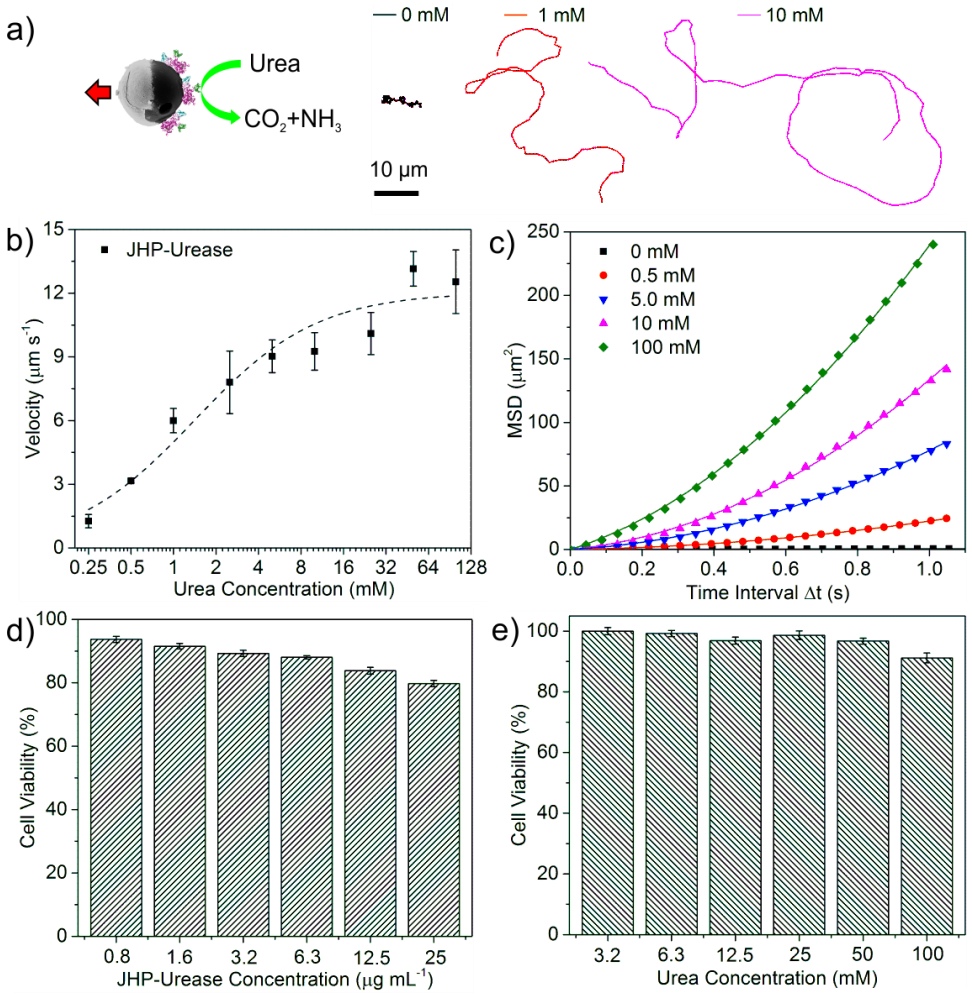

Figure 3. Directional motion of the biocompatible microcapsule motor driven by non-toxic/biological fuel of urea. a) Schematic illustration of the urea driven microcapsule motor and typical tracking trajectories at different fuel concentrations up to 30 s; b) velocity of the

microcapsule motor versus fuel concentration (Statistics were obtained by measuring velocity of 20 particles; the error bars in (b) represent standard error of mean, N=20); c) curves of mean-square-displacement (MSD) versus the time interval at varied urea concentrations (Δt); MTT cytotoxicity assay of the d) JHP-Urease and e) urea on HeLa cells (The error bars in (d) and (e) represent standard error of mean, N=8).

The self-propelled directional movement of the microcapsule motor (JHP-Urease) is powered by the bio-catalytic decomposition of urea (Figure 3a). The asymmetric reaction continuously consumes urea in the solution while producing the new chemical species CO_2 and NH_3, however, only at the non-coated face of the Janus particle. This induces a concentration gradient and active directional flow of these chemical species around the particle surface, resulting in a self-generated diffusiophoresis (i.e., forward momentum in the direction away from the uncoated hemisphere) of the Janus particles.[18] The velocity of the microcapsule was calculated by measuring the length of the particle trajectory in a defined time period (>10 s), based on optical video recordings with a frame rate of 20 fps. Typical tracking trajectory of the microcapsule motor at 0 mM urea exhibit Brownian motion only, while those with presence of urea, e.g. 1 mM and 10 mM, indicate active self-propulsion (Figure 3a). Videos showing the directional movement of active microcapsule motors at 1 mM and 100 mM urea are provided (Supporting Video S1 and S2 in the SI). The average velocity of the microcapsule motors is positively correlated with the urea concentration, indicating fuel concentration dependent enzymatic activity. According to Michaelis–Menten enzyme kinetics, the enzymatic reaction rate can be calculated from $V=V_{max}[S]/K_m+[S]$, where K_m is the Michaelis constant, [S] is the substrate (urea) concentration, V_{max} is the maximum reaction rate. The velocity exhibits a linear

dependence on the urea concentration for low urea concentrations of up to 10 mM, which agrees with the Michaelis–Menten enzymatic kinetics provided that values for K_m are within the range of 2-5 mM.[13] The reaction rate should begin to saturate when substrate concentration [S] reaches 50 mM ($\geq 10K_m$), which should in turn affect the particle velocities. In good agreement with this theoretical prediction, we found that the microcapsule motors also reached their maximal velocities of about 12 μm s^{-1} (6 body lengths s^{-1}) at concentrations of about 50 mM (Figure 3b). These velocity values of our microcapsule motors are comparable to velocities observed in phoretic motions of Janus spherical micro-motors that are driven by Pt/H_2O_2.[19] The fit obtained from the Michaelis–Menten enzyme kinetics equation matches the observed velocity values quite well (Figure 3b), suggesting that the active motion of the microcapsule is directly correlated to the enzyme activity of immobilized urease on the Janus particle's surface.

Based on the extracted coordinates (x μm, y μm) along the particle trajectories, we calculated the mean-square-displacement (MSD) at different urea concentrations as a function of time interval (Δt) (Figure 3c). As the fuel availability was increased, the MSD curves showed an increasingly parabolic shape, indicating a transition from diffusive to ballistic motion of the micro-motors.[19] We observed higher chances of directional change as well as circling behavior for the microcapsule motors compared to common Janus spherical micro-motors powered by Pt/H_2O_2. This might be linked to the non-homogenous coating of enzymes and additional symmetry-breaking effects due to the randomly distributed large holes on the particle surface, which may have introduced asymmetries in the self-propulsion force.

Furthermore, we evaluated the cytotoxicity of the JHP-Urease and fuel urea with HeLa cell lines by (3-(4,5-dimethylthiazol-2-yl)-2,5-diphenyltetrazolium bromide) (MTT) assay. Both the microcapsule and fuel urea demonstrated non-toxic effect towards HeLa cells up to high

concentrations of 32 μg mL^{-1} and 100 mM, respectively (Figure 3d and e). The normal concentration of urea in human blood is about 5-10 mM and of the order of hundreds of mM in human urine,[20] and the microcapsule motors could move at an average velocity of about 3 μm s^{-1} with urea concentrations as low as 0.5 mM, thus we accomplished a biocompatible microcapsule motors that can be self-propelled by biologically available fuel at physiological concentrations.

The mesoporous hollow structure enables the microcapsule to act as a micro cargo delivery system with multiple cargo loading capability. As a first step, we needed to establish whether the microcapsule was capable to carry small therapeutic agents. This could be demonstrated by mixing the HP with Dox aqueous solution (1 mg mL^{-1}) for 24 h. During this period, the Dox molecules became encapsulated into the mesopores through free diffusion.[21] Under fluorescent lighting the loaded Dox appear as circular red dots inside the HP shell (Figure S7a in the SI). In addition, the presence of large holes in the capsules' surface could facilitate the encapsulation of larger cargo, such as proteins, nucleic acid, and even functional nanoparticles.[22] To prove this point, we successfully loaded SiO_2 nanoparticles with a diameter of 350 nm into the hollow capsules (Figure S7b in the SI).

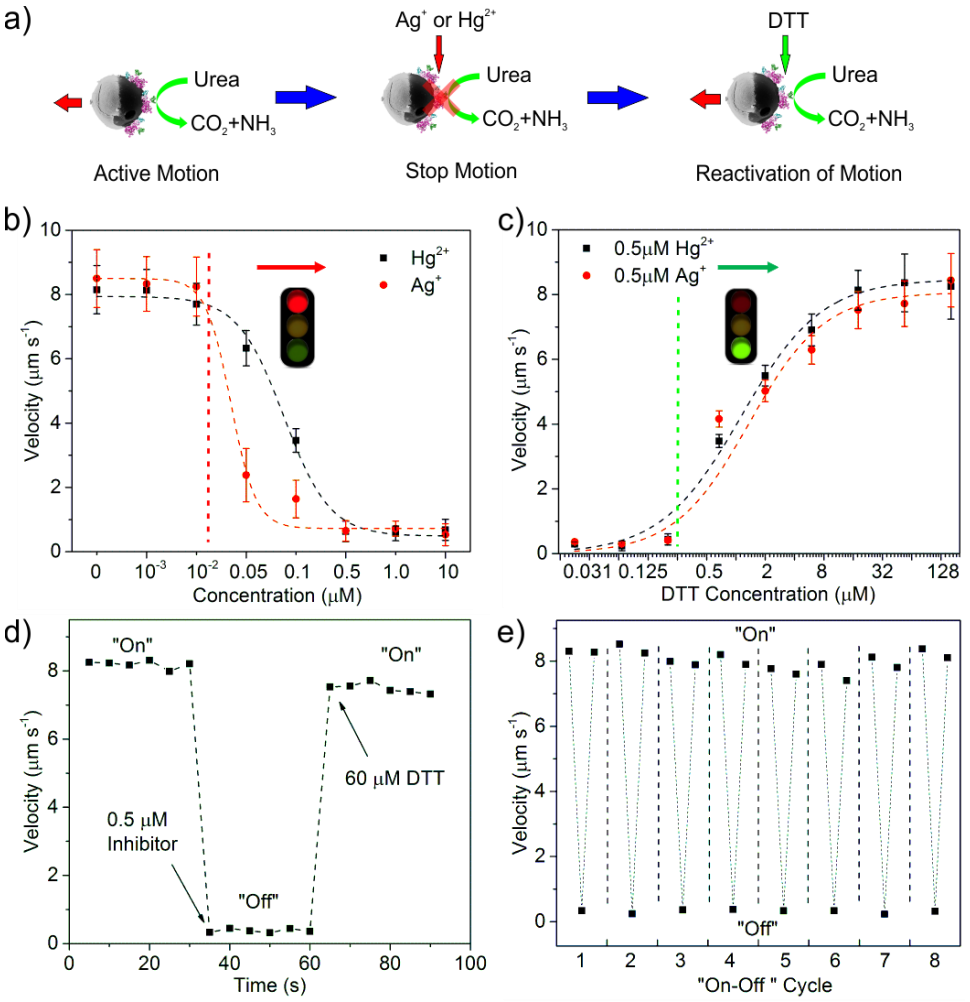

Figure 4. Velocity control on the microcapsule motor by manipulating the enzymatic activity of urease. a) Schematic illustration of the velocity control by inhibiting/reactivating enzyme activity; b) velocity of the microcapsule motor at 50 mM urea as a function of inhibitors (Ag^{+} or Hg^{2+}) concentration; c) velocity of the microcapsule motor at 50 mM urea and 0.5 μM inhibitors as a function of DTT concentration; (Statistics were obtained by measuring velocity of 20 particles; the error bars represent standard error of mean, N=20.) d) Real time "On-Off" motion control by addition of inhibitor (Ag^{+} or Hg^{2+}) and DTT; and e) Repeatability of "On-Off" motion up to eight cycles.

Since the mechanical force necessary for the self-propulsion of the microcapsule is directly related to the enzymatic activity of urease, we can control the velocity of the microcapsule motor by manipulating its enzymatic activity (Figure 4a). Ag^{+} and Hg^{2+} are strong inhibitors of urease by forming a urease-inhibitor complex.[13] This inhibition process is reversible and the enzymatic activity of urease can be reactivated by a thiol protecting agent, such as DTT to form the DTT-inhibitor complex trough competitive binding.[13b] Upon addition of inhibitor (Ag^{+} or Hg^{2+}), we were able to decrease the velocity of the microcapsule motor and completely stop its directional movement once the concentration of inhibitor reached 0.5 μM (Figure 4b). In order to re-activate the micro-motor, we first placed it in a solution containing 50 mM urea and 0.5 μM inhibitor (Ag^{+} or Hg^{2+}) which inhibited all enzymatic activity and led to a complete stop of the micro-motor, effectively leaving it in "stand-by" mode. By adding DTT, the microcapsule motor was quickly re-activated and we observed a rapid increase in its velocity (Figure 4c). In parallel, we evaluated the enzymatic activity of JHP-Urease in the same conditions by measuring the generation of ammonia. We found a similar trend of decreasing enzymatic activity for increased concentrations of inhibitors (Figure S8a in the SI). As before, the enzymatic activity of the JHP-Urease was restored upon addition of DTT (Figure S8b in the SI). Both results indicate that the self-propulsion of the microcapsule motor is driven by enzymatic activity.

We even demonstrated the existence of an instantaneous "On-Off" motion control of the microcapsule motor in real time, analogous to switching a macroscopic engine on or off. Initially, the microcapsule motor showed the typical directional self-propulsion with presence of urea; upon addition of 0.5 μM inhibitor (Ag^{+} or Hg^{2+}), we successfully "switched off" the enzymatic "engine" and stopped the microcapsule motor, while subsequent addition of 60 μM of DTT led to an immediate re-activation of the microcapsule motor (Figure 4d). During the stop-

phase, the bio-catalytic reaction of decomposition of urea had also completely stopped (Figure S8c in the SI). A supporting video S3 in the SI is provided, showing the instant "On-Off" motion upon addition of inhibitor and DTT. It is worth mention that the micro-motors have good reusability and the "On-Off" motion control cycle is repeatable. After reactivation of the micro-motors, we collected the motors by centrifugation and washed with DI H_2O to remove the inhibitors and DTT. Then, we repeated the chemically manipulated "On-Off" motion control cycle without apparent loss in velocity up to eight cycles as demonstrated in Figure 4e. We further examined the cytotoxicity of the inhibitors (Ag^+ or Hg^{2+}) used here by carrying out MTT assay with HeLa cell lines (Figure S9 in the SI). At the inhibitors' effective concentration (about 0.5 μM), no obvious toxic effect was observed, which can ensure the biocompatibility of the whole system. Nevertheless, Ag^+ ion is preferred as inhibitor to control the motor's motion in biomedical applications, considering possible harmful effect of Hg^{2+} towards living organism. In addition to active cargo delivery in biomedical applications, sensitivity of the motor's velocity towards heavy metals, such as Hg^{2+}, enables the motors to serve as "on-the-fly" active sensor for heavy metal detection in environmental application, which was demonstrated by previous researcher as well.[5b]

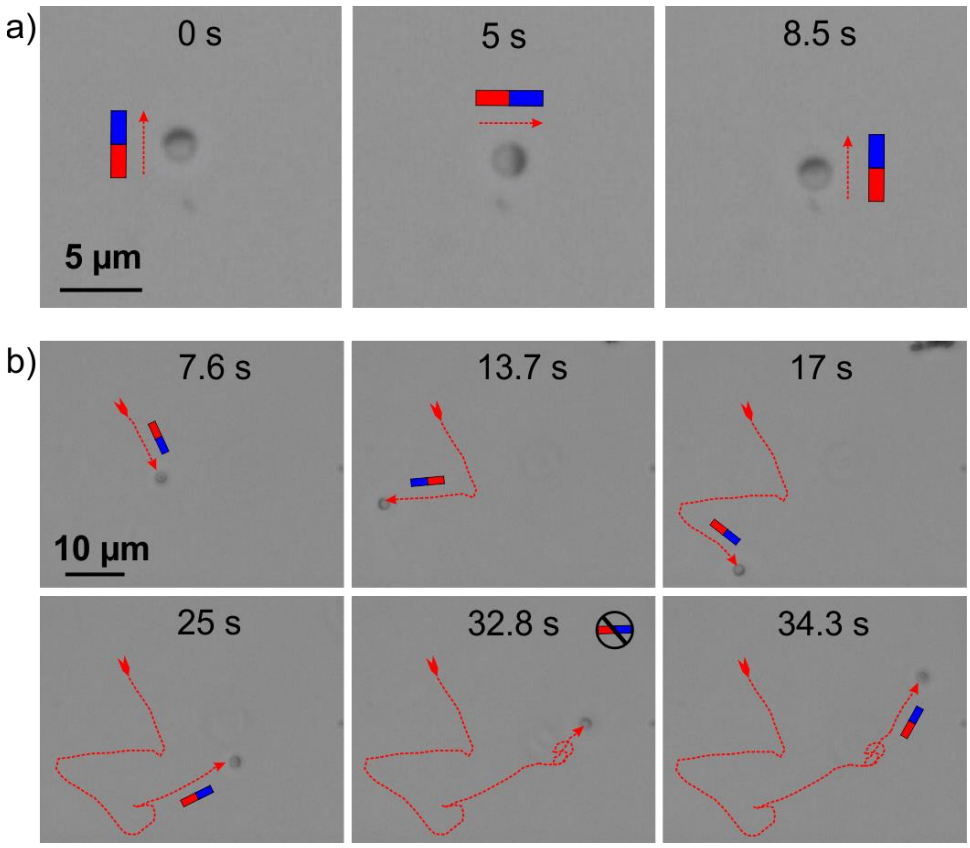

Figure 5. a) Remote magnetic control on the orientation of JHP-Urease microcapsule motor. From left to right are video snap-shot images of micro-motor placed in aqueous without urea fuel and under different magnetic field orientation (Supporting Video S4 in the SI); b) Magnetic guidance on the movement direction of the JHP-Urease microcapsule motor. From left to right are snap-shot images of the micro-motor with urea fuel at different times (Supporting Video S5 in the SI).

In addition to velocity manipulation, directional guidance of the carrier is necessary for future target cargo delivery applications. In previous reports, a magnetic field was employed to control the direction of movement of micro-motors, including micro- tubes,[23] nano-wires[24] and Janus particles.[25] Here, we first deposited a layer of the element Fe (10 nm) for magnetic control, followed by a second layer of Au (3 nm) to protect the Fe from dissolving into the aqueous

solution and also allows for future biomedical functionalization through Au-S linkage. In order to be able to investigate the orientation control in the absence of self-propelled motion, we placed the magnetic microcapsule motor in aqueous solution without any fuel. We could induce orientation changes (turning angles of $\Delta\theta=90°$) of the microcapsule motor by changing the direction of the magnetic field with a strength of about 100 mT (Figure 5a and Supporting Video S4 in the SI). However, in the absence of self-propulsion the application of a magnetic field alone, only resulted in orientation changes of the microcapsule motor but did not lead to any displacement or directed movement of the particle. Then, we demonstrated magnetic guidance on active micro-motors. The magnetic microcapsule motor with metallic coating could also move actively (Figure 5 b and Supporting Video S5 in the SI). When an external magnetic field was applied, the direction of motion of the magnetic microcapsule motor aligned with the direction of the magnetic field lines, which in our case led to movement in a straight line (Figure 5b). By changing the polarity of the magnetic field, the direction of movement of the magnetic microcapsule motor was reversed accordingly. To better illustrate the effect of the magnetic forcing on the movement direction, we temporarily switched off the magnetic field at time 32.8 s which resulted in a more circular trajectory of the microcapsule motor, possibly due to asymmetries in the propulsion force (see above). Once we re-applied the magnetic field, the microcapsule motor would resume its guided motion and move in a straight line again. The magnetic field thus only acts as the steering wheel of the microcapsule motor while the momentum is produced by the enzymatic reactions. We thus accomplished to exert complete motion control on the micro-motor: it could be oriented, slowed, accelerated, or brought to a complete stop and subsequently re-activated at will.

In summary, we presented a fully biocompatible active micro-motor, made of non-toxic silica and fueled by biologically available urea, one of the most promising platforms for future biomedical applications of active micro/nano-machines. We demonstrated complete motion control of the self-propelled hollow microcapsule motor: the velocity was controlled by chemically altering the enzymatic activity of urease while the direction was controlled by using a magnetic element to construct the Janus structure and applying an external magnetic field. The ability of encapsulating multiple cargos into the mesoporous hollow particles allows for the transportation of cargo of different sizes by the microcapsule motor to target locations on-demand, leading to novel possibilities for targeted drug delivery in biomedical applications. Future investigation on collective behavior or alternative guidance methods such as chemotaxis, pH-taxis, and thermos-taxis will be of great potential for constructing intelligent, biologically benign micro-systems based on the active microcapsules.

ASSOCIATED CONTENT

Supporting Information. Experimental details, characterization of mesoporous structure of the hollow capsule, characterization results of enzyme conjugation and protein quantification, MTT cytotoxicity assay, inhibition and re-activation of enzymatic activity of the JHP-Urease, magnetic control on the orientation of the Janus motors, and supporting videos are included in the Supporting Information. This material is available free of charge via the Internet at http://pubs.acs.org.

AUTHOR INFORMATION

Corresponding Author

Samuel Sanchez

* Email: sanchez@is.mpg.de

Author Contributions

The manuscript was written through contributions of all authors. All authors have given approval to the final version of the manuscript.

ACKNOWLEDGMENT

Authors thank Prof. P. Fischer for instruments support. The research leading to these results has received funding from the European Union Seventh Framework Program [FP/2007/2013] under grant agreement no. 312483 (ESTEEM2), European Research Council under the European Union's Seventh Framework Program (FP7/20072013)/ERC grant agreement no. 311529 (LT-NRBS), and the Alexander von Humboldt Foundation.

REFERENCES

1. (a) Sengupta, S.; Ibele, M. E.; Sen, A., Fantastic Voyage: Designing Self-Powered Nanorobots. *Angewandte Chemie-International Edition* **2012,** *51* (34), 8434-8445; (b) Wang, H.; Pumera, M., Fabrication of Micro/Nanoscale Motors. *Chemical Reviews* **2015**; (c) Sánchez, S.; Soler, L.; Katuri, J., Chemically Powered Micro- and Nanomotors. *Angewandte Chemie International Edition* **2015,** *54* (5), 1414-1444; (d) Wang, J., *Nanomachines: Fundamentals and Applications*. Wiley-VCH: Weinheim, 2013.
2. (a) Guix, M.; Mayorga-Martinez, C. C.; Merkoçi, A., Nano/Micromotors in (Bio)chemical Science Applications. *Chemical Reviews* **2014,** *114* (12), 6285-6322; (b) Wang, J.; Gao, W., Nano/Microscale Motors: Biomedical Opportunities and Challenges. *Acs Nano* **2012,** *6* (7), 5745-5751; (c) Abdelmohsen, L.; Peng, F.; Tu, Y. F.; Wilson, D. A., Micro- and nano-motors for biomedical applications. *Journal of Materials Chemistry B* **2014,** *2* (17), 2395-2408.
3. Gardner, A. M.; Xu, F.-h.; Fady, C.; Jacoby, F. J.; Duffey, D. C.; Tu, Y.; Lichtenstein, A., Apoptotic vs. Nonapoptotic Cytotoxicity Induced by Hydrogen Peroxide. *Free Radical Biology and Medicine* **1997,** *22* (1–2), 73-83.
4. (a) Gao, W.; Uygun, A.; Wang, J., Hydrogen-Bubble-Propelled Zinc-Based Microrockets in Strongly Acidic Media. *Journal of the American Chemical Society* **2012,** *134* (2), 897-900; (b) Gao, W.; D'Agostino, M.; Garcia-Gradilla, V.; Orozco, J.; Wang, J., Multi-Fuel Driven Janus Micromotors. *Small* **2013,** *9* (3), 467-471; (c) Gao, W.; Pei, A.; Dong, R. F.; Wang, J., Catalytic

Iridium-Based Janus Micromotors Powered by Ultralow Levels of Chemical Fuels. *Journal of the American Chemical Society* **2014,** *136* (6), 2276-2279; (d) Gao, W.; Pei, A.; Wang, J., Water-Driven Micromotors. *Acs Nano* **2012,** *6* (9), 8432-8438; (e) Mou, F. Z.; Chen, C. R.; Ma, H. R.; Yin, Y. X.; Wu, Q. Z.; Guan, J. G., Self-Propelled Micromotors Driven by the Magnesium-Water Reaction and Their Hemolytic Properties. *Angew. Chem., Int. Ed.* **2013,** *52* (28), 7208-7212; (f) Moo, J. G. S.; Wang, H.; Pumera, M., Acetylene bubble-powered autonomous capsules: towards in situ fuel. *Chemical communications* **2014,** *50* (100), 15849-15851; (g) Wang, H.; Sofer, Z.; Eng, A. Y. S.; Pumera, M., Iridium-Catalyst-Based Autonomous Bubble-Propelled Graphene Micromotors with Ultralow Catalyst Loading. *Chemistry – A European Journal* **2014,** *20* (46), 14946-14950.

5. (a) Sanchez, S.; Solovev, A. A.; Mei, Y.; Schmidt, O. G., Dynamics of Biocatalytic Microengines Mediated by Variable Friction Control. *Journal of the American Chemical Society* **2010,** *132* (38), 13144-13145; (b) Orozco, J.; Garcia-Gradilla, V.; D'Agostino, M.; Gao, W.; Cortes, A.; Wang, J., Artificial Enzyme-Powered Microfish for Water-Quality Testing. *Acs Nano* **2013,** *7* (1), 818-824.

6. (a) Wu, Y.; Lin, X.; Wu, Z.; Möhwald, H.; He, Q., Self-Propelled Polymer Multilayer Janus Capsules for Effective Drug Delivery and Light-Triggered Release. *ACS Applied Materials & Interfaces* **2014,** *6* (13), 10476-10481; (b) Ma, X.; Sanchez, S., A bio-catalytically driven Janus mesoporous silica cluster motor with magnetic guidance. *Chemical communications* **2015,** *51* (25), 5467-5470; (c) Simmchen, J.; Baeza, A.; Ruiz, D.; Esplandiu, M. J.; Vallet-Regí, M., Asymmetric Hybrid Silica Nanomotors for Capture and Cargo Transport: Towards a Novel Motion-Based DNA Sensor. *Small* **2012,** *8* (13), 2053-2059.

7. (a) Sengupta, S.; Dey, K. K.; Muddana, H. S.; Tabouillot, T.; Ibele, M. E.; Butler, P. J.; Sen, A., Enzyme Molecules as Nanomotors. *Journal of the American Chemical Society* **2013,** *135* (4), 1406-1414; (b) Bunea, A.-I.; Pavel, I.-A.; David, S.; Gáspár, S., Sensing based on the motion of enzyme-modified nanorods. *Biosensors and Bioelectronics* **2015,** *67*, 42-48.

8. Sengupta, S.; Patra, D.; Ortiz-Rivera, I.; Agrawal, A.; Shklyaev, S.; Dey, K. K.; Cordova-Figueroa, U.; Mallouk, T. E.; Sen, A., Self-powered enzyme micropumps. *Nature Chemistry* **2014,** *6* (5), 415-422.

9. (a) Mano, N.; Heller, A., Bioelectrochemical Propulsion. *Journal of the American Chemical Society* **2005,** *127* (33), 11574-11575; (b) Pantarotto, D.; Browne, W. R.; Feringa, B. L., Autonomous propulsion of carbon nanotubes powered by a multienzyme ensemble. *Chemical communications* **2008,** (13), 1533-1535.

10. (a) Ma, X.; Jannasch, A.; Albrecht, U.-R.; Hahn, K.; Miguel-López, A.; Schäffer, E.; Sánchez, S., Enzyme-Powered Hollow Mesoporous Janus Nanomotors. *Nano Letters* **2015,** *15* (10), 7043-7050; (b) Dey, K. K.; Zhao, X.; Tansi, B. M.; Méndez-Ortiz, W. J.; Córdova-Figueroa, U. M.; Golestanian, R.; Sen, A., Micromotors Powered by Enzyme Catalysis. *Nano Letters* **2015,** *15* (12), 8311-8315; (c) Schattling, P.; Thingholm, B.; Städler, B., Enhanced Diffusion of Glucose-Fueled Janus Particles. *Chemistry of Materials* **2015,** *27* (21), 7412-7418.

11. (a) Li, Z.; Barnes, J. C.; Bosoy, A.; Stoddart, J. F.; Zink, J. I., Mesoporous silica nanoparticles in biomedical applications. *Chemical Society Reviews* **2012,** *41* (7), 2590-2605; (b) Slowing, I. I.; Vivero-Escoto, J. L.; Wu, C.-W.; Lin, V. S. Y., Mesoporous silica nanoparticles as controlled release drug delivery and gene transfection carriers. *Advanced Drug Delivery Reviews* **2008,** *60* (11), 1278-1288.

12. Trewyn, B. G.; Slowing, I. I.; Giri, S.; Chen, H.-T.; Lin, V. S. Y., Synthesis and Functionalization of a Mesoporous Silica Nanoparticle Based on the Sol–Gel Process and Applications in Controlled Release. *Accounts of Chemical Research* **2007,** *40* (9), 846-853.
13. (a) Du, N.; Chen, M.; Liu, Z.; Sheng, L.; Xu, H.; Chen, S., Kinetics and mechanism of jack bean urease inhibition by Hg(2+). *Chemistry Central Journal* **2012,** *6*, 154-154; (b) Krajewska, B.; Zaborska, W.; Chudy, M., Multi-step analysis of Hg2+ ion inhibition of jack bean urease. *Journal of Inorganic Biochemistry* **2004,** *98* (6), 1160-1168.
14. Qi, G.; Wang, Y.; Estevez, L.; Switzer, A. K.; Duan, X.; Yang, X.; Giannelis, E. P., Facile and Scalable Synthesis of Monodispersed Spherical Capsules with a Mesoporous Shell. *Chemistry of Materials* **2010,** *22* (9), 2693-2695.
15. Zhang, X.; Guan, R.-F.; Wu, D.-Q.; Chan, K.-Y., Enzyme immobilization on amino-functionalized mesostructured cellular foam surfaces, characterization and catalytic properties. *Journal of Molecular Catalysis B: Enzymatic* **2005,** *33* (1–2), 43-50.
16. Mahmoudi, M.; Lynch, I.; Ejtehadi, M. R.; Monopoli, M. P.; Bombelli, F. B.; Laurent, S., Protein−Nanoparticle Interactions: Opportunities and Challenges. *Chemical Reviews* **2011,** *111* (9), 5610-5637.
17. (a) Sharma, B.; Mandani, S.; Sarma, T. K., Biogenic Growth of Alloys and Core-Shell Nanostructures Using Urease as a Nanoreactor at Ambient Conditions. *Sci. Rep.* **2013,** *3*; (b) Cruz, J. C.; Pfromm, P. H.; Tomich, J. M.; Rezac, M. E., Conformational changes and catalytic competency of hydrolases adsorbing on fumed silica nanoparticles: II. Secondary structure. *Colloids and Surfaces B: Biointerfaces* **2010,** *81* (1), 1-10.
18. (a) Wang, W.; Duan, W. T.; Ahmed, S.; Mallouk, T. E.; Sen, A., Small power: Autonomous nano- and micromotors propelled by self-generated gradients. *Nano Today* **2013,** *8* (5), 531-554; (b) Thakur, S.; Kapral, R., Dynamics of self-propelled nanomotors in chemically active media. *Journal of Chemical Physics* **2011,** *135* (2); (c) Golestanian, R.; Liverpool, T. B.; Ajdari, A., Propulsion of a Molecular Machine by Asymmetric Distribution of Reaction Products. *Phys. Rev. Lett.* **2005,** *94* (22), 220801.
19. (a) Howse, J. R.; Jones, R. A.; Ryan, A. J.; Gough, T.; Vafabakhsh, R.; Golestanian, R., Self-Motile Colloidal Particles: from Directed Propulsion to Random Walk. *Phys. Rev. Lett.* **2007,** *99* (4), 048102; (b) Dunderdale, G.; Ebbens, S.; Fairclough, P.; Howse, J., Importance of Particle Tracking and Calculating the Mean-Squared Displacement in Distinguishing Nanopropulsion from Other Processes. *Langmuir* **2012,** *28* (30), 10997-11006.
20. MacKay, E. M.; MacKay, L. L., THE CONCENTRATION OF UREA IN THE BLOOD OF NORMAL INDIVIDUALS. *Journal of Clinical Investigation* **1927,** *4* (2), 295-306.
21. Ma, X.; Zhao, Y.; Ng, K. W.; Zhao, Y., Integrated Hollow Mesoporous Silica Nanoparticles for Target Drug/siRNA Co-Delivery. *Chemistry – A European Journal* **2013,** *19* (46), 15593-15603.
22. Hyuk Im, S.; Jeong, U.; Xia, Y., Polymer hollow particles with controllable holes in their surfaces. *Nat Mater* **2005,** *4* (9), 671-675.
23. Solovev, A. A.; Sanchez, S.; Pumera, M.; Mei, Y. F.; Schmidt, O. G., Magnetic Control of Tubular Catalytic Microbots for the Transport, Assembly, and Delivery of Micro-objects. *Advanced Functional Materials* **2010,** *20* (15), 2430-2435.
24. Kline, T. R.; Paxton, W. F.; Mallouk, T. E.; Sen, A., Catalytic nanomotors: Remote-controlled autonomous movement of striped metallic nanorods. *Angew. Chem., Int. Ed.* **2005,** *44* (5), 744-746.

25. Baraban, L.; Makarov, D.; Streubel, R.; Mönch, I.; Grimm, D.; Sanchez, S.; Schmidt, O. G., Catalytic Janus Motors on Microfluidic Chip: Deterministic Motion for Targeted Cargo Delivery. *ACS Nano* **2012,** *6* (4), 3383-3389.

Insert Table of Contents Graphic and Synopsis Here

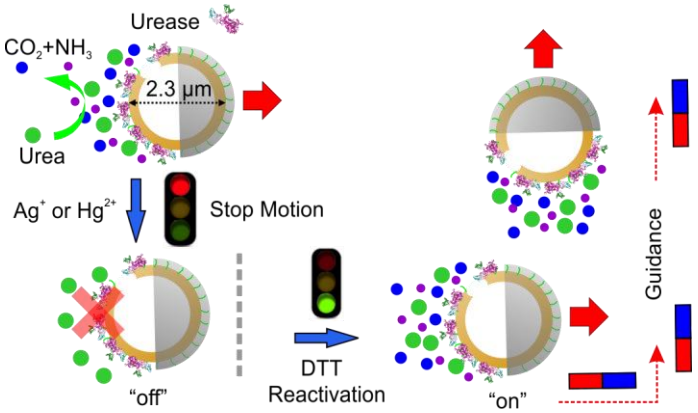

We present a fully controllable microcapsule motors capable of long-range self-propulsion, consuming biocompatible fuel of urea. By inhibiting and re-activating the enzymatic activity, we can control the velocity of the micro-motors. Directional guidance of the microcapsule motor is accomplished with incorporation of magnetic element into the Janus structure. Plus multiple cargo loading capability, the hybrid microcapsule motor provides a promising active drug delivery micro-system in future biomedical applications.